References

[1] Seiff, A. and Reese, D. E., Jr., "Defining Mars' Atmosphere—a Goal for Early Missions," *Astronautics and Aeronautics*, Vol. 3, No. 2, Feb. 1965, pp. 16–21.

[2] Peterson, V. L., "A Technique for Determining Planetary Atmosphere Structures for Measured Accelerations of an Entry Vehicle," TN D-2669, 1965, NASA.

[3] Sommer, S. C., Boissevain, A. G., Yee, L., and Hedlund, R. C., "The Structure of an Atmosphere from On-Board Measurements of Pressure, Temperature, and Acceleration," TN D-3933, 1967, NASA.

[4] Seiff, A., Reese, D. E., Sommer, S. C., Kirk, D. B., Whiting, E. E., and Niemann, H. B., "PAET, an Entry Probe Experiment in the Earth's Atmosphere," *Icarus*, Vol. 18, No. 4, April 1973, pp. 525–563.

[5] DeRose, C. E., "Trim Attitude, Lift and Drag of the Apollo Command Module with Offset Center-of-Gravity Positions at Mach Numbers to 29," TN D-5276, 1969, NASA.

[6] Sammonds, R. I., "Aerodynamics of Mars Entry Probe-Lander Configurations at a Mach Number of 10," TN D-5608, 1970, NASA.

[7] Sammonds, R. I., "Dynamics of High-Drag Probe Shapes at Transonic Speeds," TN D-6489, 1971, NASA.

[8] Campbell, J. F., "Longitudinal Aerodynamic Characteristics of Several High-Drag Bodies at Mach Numbers from 1.50 to 4.63," TN D-3915, 1967, NASA.

[9] Campbell, J. F. and Howell, D. T., "Supersonic Aerodynamics of Large-Angle Cones," TN D-4719, 1968, NASA.

[10] Campbell, J. F., "Supersonic Aerodynamic Characteristics and Shock Standoff Distances for Large-Angle Cones with and without Cylindrical Afterbodies," TN D-5334, 1969, NASA.

[11] Campbell, J. F. and Howell, D. R., "Supersonic Lifting Capabilities of Large-Angle Cones," TN D-5499, 1969, NASA.

[12] South, J. C., Jr., "Calculation of Axisymmetric Supersonic Flow Past Blunt Bodies with Sonic Corners, Including a Program Description and Listing," TN D-4563, 1968, NASA.

[13] Nichols, J. and Nierengarten, E., "Static Aerodynamic Characteristics of Blunted Cones and Round-Shouldered Cylinders Suitable for Planetary Entry Vehicles at a Mach-Number Range 1.65 to 9.00," JPL WT20-558, 1964.

[14] Nichols, J. O. and Nierengarten, E. A., "Aerodynamic Characteristics of Blunt Bodies," JPL TR32-677, 1965.

[15] Walker, B. and Weaver, R. W., "Static Aerodynamic Characteristics of Blunted Cones in the Mach-Number Range from 2.2 to 9.5," JPL TR32-1213, 1967.

[16] Canning, T. N., Seiff, A., and James, C. S., eds., "Ballistic Range Technology," AGARDograph 138, Chap. 2, Aug. 1970.

[17] Malcolm, G. N. and Chapman, G. T., "A Computer Program for Systematically Analyzing Free-Flight Data to Determine the Aerodynamics of Axisymmetric Bodies," TN D-4766, 1968, NASA.

[18] Rasmussen, M. L. and Kirk, D. B., "On the Pitching and Yawing Motion of a Spinning Symmetric Missile Governed by an Arbitrary Nonlinear Restoring Moment," TN D-2135, 1964, NASA.

[19] Canning, T. N., Seiff, A., and James, C. S., eds., "Ballistic Range Technology," AGARDograph 138, Chap. 7, Aug. 1970.

JANUARY 1975 J. SPACECRAFT VOL. 12, NO. 1

Attitude Time-Series Estimator for Rectification of Spaceborne Imagery

R. H. CARON* AND K. W. SIMON†
TRW Systems Group, Redondo Beach, Calif.

Unprocessed digital multispectral imagery from the ERTS-1 satellite exhibits distortions due to fluctuations in the spacecraft's attitude. These distortions are easily removed if the attitude time-series of the spacecraft can be estimated with sufficient precision. A solution to this estimation problem is offered in the form of a discrete-time, sequential, mean-square-sense optimal estimator which uses ground control point observables. A computer implementation and performance evaluation using ERTS-1 data is discussed.

Nomenclature

ERTS	= Earth Resources Technology Satellite
MSS	= multispectral scanner
BIAT	= bulk image annotation tape
GCP	= ground control point (observation)
ICT	= image center time
ECR	= earth-centered rotating (coordinate system)
pixel	= picture element
$\mathbf{R}_G$	= ECR position of a GCP
$\Psi = (\Psi_r, \Psi_p, \Psi_y)$	= attitude time-series coefficient vector
$\sigma = (\mathbf{R}_S, \mathbf{V}_S)$	= ephemeris time-series vector
β	= mirror scan angle time-series
t	= time
ϕ	= MSS detector deployment angle
$\mathbf{n}$	= observation noise vector
$\theta = (\theta_r, \theta_p, \theta_y)$	= attitude time-series vector
δ	= distance between the spacecraft and a GCP
$\mathbf{u}$	= MSS unit scan vector in ECR
$\|\cdot\|$	= Euclidean norm
$\lvert\cdot\rvert$	= absolute value operator
$\mathbf{R}, \mathbf{P}, \mathbf{Y}$	= local orbit-based coordinates
∇_q	$= \left[\frac{\partial}{\partial q_1}, \ldots, \frac{\partial}{\partial q_n}\right]^T$ = matrix partial differentiation operator
$\lfloor x \rfloor$	= greatest integer not exceeding x
$\hat{\Psi}$	= estimator of Ψ
$A(k)$	= optimal gain matrix
$P(k)$	= estimator error covariance matrix
$\Lambda(k)$	= covariance matrix of $\mathbf{n}$
ε_p	= norm of the position estimation error
C	= cosine
S	= sine

Received May 22, 1974; revision received August 26, 1974. The authors are indebted to M. Byerly of the U.S. Geological Survey, who supplied the precision geodetic inputs necessary to evaluate the estimator, and B. Peavey of NASA/GSFC, who provided technical information relative to the ERTS-1 system.

Index categories: Computer Technology and Computer Simulation Techniques; Data Sensing and Presentation or Transmission Systems; Spacecraft Attitude Dynamics and Control.

* Member Technical Staff.

† Section Head.

I. Introduction

A PROPERTY of unprocessed (bulk) digital ERTS-1 multispectral scanner (MSS) imagery is that it contains distortion due to a continually changing spacecraft attitude during image scan. This distortion can be removed using the TRW image rectification process wherein models of the MSS system and spacecraft dynamics are used to project a bulk image onto some geodetic coordinate system such as Universal Transverse Mercator.[1] In particular, this process requires an estimate of the ERTS attitude time-series over the time interval in which the image was scanned. Such an estimate can be obtained by fitting polynomials to the attitude sampled data on the Bulk Image Annotation Tape (BIAT) which NASA supplies with its bulk imagery.[2,3] Unfortunately, when image rectification is required with one picture element (pixel) precision, an estimate obtained in this fashion proves to be inadequate: To achieve one pixel rectification, each attitude component should be known to the nearest tenth of a milliradian; however, the ERTS-1 attitude measurement system is only accurate to the nearest milliradian.[4] It follows that some additional information is required to obtain a more refined estimate.

The approach to attitude time-series estimation described here consists of using Ground Control Point (GCP) observables in conjunction with a discrete-time sequential estimator. More specifically, suppose that the ERTS attitude time series (restricted to the image time interval) is represented by a random vector $\Psi = (\Psi_r^T, \Psi_p^T, \Psi_y^T)^T$, whose subvector components are comprised of sets of coefficients which define polynomial realizations of the roll, pitch, and yaw time-series, respectively. Next, consider a GCP to be in the form of a vector $\mathbf{R}_G$ in some geocentric coordinate system, and suppose that the GCP qua $\mathbf{R}_G$ is imaged by the MSS at Image Center Time (ICT)‡ t. Then, in the absence of observation uncertainty, $\mathbf{R}_G$ is related to Ψ and t via a nonlinear transformation $\mathbf{G}(\Psi;\ \sigma,\ \beta,\ t,\ \phi)$, where $\sigma = (\mathbf{R}_S^T, \mathbf{V}_S^T)^T$ is the ERTS ephemeris time-series, β is the MSS mirror scan angle time-series and ϕ is the deployment angle associated with the MSS detector that imaged the GCP. Assuming an additive white Gaussian observation noise model $\mathbf{n}$, $\mathbf{R}_G$ can be modeled as a value of a sample from the parameter dependent Gaussian stochastic process

$$\mathbf{R}_G(t) = \mathbf{G}(\Psi;\sigma,\beta,t,\phi)+\mathbf{n}(t) \tag{1}$$

Below, we discuss the design, implementation and performance evaluation of a discrete-time sequential estimator of Ψ which uses for its observables the values of $\mathbf{R}_G$ over a finite set of time instants.

II. Derivation of the Transformation G

An Earth-Centered Rotating (ECR) 3-D right-hand coordinate system (with x-axis passing through the Greenwich Meridian at the equator) was chosen to reference the GCP observables. This choice was predicted upon two factors: 1) a simple explicit form for $\mathbf{G}$ is easily derived in this system; and 2) for the range of deviations from nominal attitude experienced by ERTS (less than 10 mrad/component), the second and higher order terms in the Taylor's expansion of the $\mathbf{G}$ so derived prove to be negligible. The significance of the second factor is that a locally linear $\mathbf{G}$ is necessary if certain well-known results in classical estimation theory are to be applicable.

The derivation of $\mathbf{G}$ is straightforward when the actual attitude time-series $\theta = (\theta_r, \theta_p, \theta_y)^T$ is used in lieu of its representation, Ψ. First, a transformation

$$\mathbf{g}(\theta;\sigma,\beta,t,\phi) = \mathbf{G}(\Psi;\sigma,\beta,t,\phi)$$

is derived, then $\mathbf{G}$ is obtained from $\mathbf{g}$ using the relationship

$$\theta_\alpha(t) = \tau_n^T(t)\Psi_\alpha,\ (\alpha\varepsilon\{r,\ p,\ y\}) \tag{2}$$

where

$$\tau_n(t) = (1,\ t,\ t^2,\ \ldots,\ t^n)^T$$

‡ ICT for a particular scene is a translation of Greenwich Meridian Time in which ICT zero occurs at the instant the geometric center of the scene is imaged by the MSS.

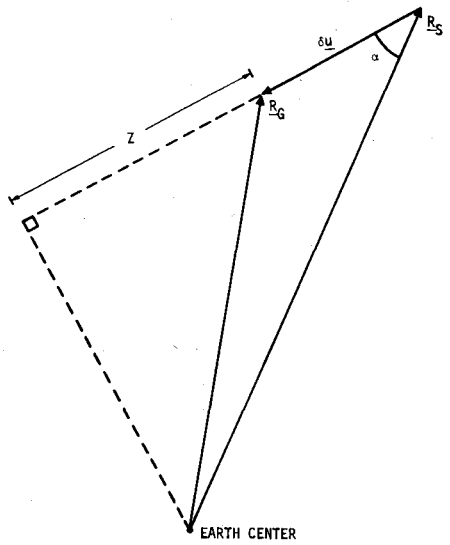

Fig. 1 ECR scan vector geometry.

assuming an nth order model for the attitude component α. The transformation $\mathbf{g}$ is most conveniently expressed in terms of the ERTS ECR position vector $\mathbf{R}_S$ and the ECR scan vector $\mathbf{u}$. The latter quantity is a unit vector pointing from $\mathbf{R}_S$ to $\mathbf{R}_G$ (cf. Fig. 1). Letting δ denote the distance between $\mathbf{R}_G$ and $\mathbf{R}_S$, it follows that

$$\mathbf{g} = \mathbf{R}_S + \delta\mathbf{u} \tag{3}$$

The scan vector $\mathbf{u}$ results from a compound transformation, applied to

$$\mathbf{1}(\beta,t,\phi) = [\sin\phi, \sin\beta(t)\cos\phi, \cos\beta(t)\cos\phi]^T \tag{4}$$

the scan vector referenced to the ERTS body coordinate system. First, $\mathbf{1}$ is mapped into the local orbit-based coordinate system via a rotation matrix $R(\theta,t)$ which accounts for the ERTS attitude at ICT t. Then $R\mathbf{1}$ is mapped into the ECR system via a coordinate transformation $E(\sigma,\ t)$ which depends upon the ERTS ephemeris at t. In summary,

$$\mathbf{u} = \mathbf{u}(\theta;\sigma,\beta,t,\phi) = E(\sigma,t)R(\theta,t)\mathbf{1}(\beta,t,\phi) \tag{5}$$

The distance δ in Eq. (3) is a function of $\mathbf{u}$, $\mathbf{R}_S$ and $\|\mathbf{R}_G\|$. Observe that

$$\mathbf{u}^T\mathbf{R}_S = -\|\mathbf{R}_S\|\cos\alpha$$

where α is the angle shown in Fig. 1. Now, since

$$\delta + z = \|\mathbf{R}_S\|\cos\alpha = -\mathbf{u}^T\mathbf{R}_S$$

if follows that

$$\delta = -\mathbf{u}^T\mathbf{R}_S - z$$

But,

$$z^2 = \|\mathbf{R}_G\|^2 - \|\mathbf{R}_S\|^2 + (\mathbf{u}^T\mathbf{R}_S)^2$$

Therefore,

$$\delta = -\mathbf{u}^T\mathbf{R}_S - (\|\mathbf{R}_G\|^2 - \|\mathbf{R}_S\|^2 + (\mathbf{u}^T\mathbf{R}_S)^2)^{1/2} \tag{6}$$

That δ depends upon $\|\mathbf{R}_G\|$ presents no difficulty since $\|\mathbf{R}_G\|$ can be approximated to within a few meters of its true value by the distance between the center of the Earth and the ERTS nadir at ICT t. This latter distance is computable using NASA-supplied nadir trajectory sampled-data in conjunction with an oblate spheroid Earth model. See Appendix A for the details of this computation.

The rotation matrix R is obtained from any compound roll, pitch, and yaw transformation carrying the ERTS body coordinates into the local orbit-based coordinates. By taking a small-angle approximation to any one of the six order-of-rotation dependent r-p-y transformations, there results a unique order-of-rotation invariant transformation.

The compound rotation of a yaw, followed by a pitch, followed by a roll is given by

$$\Omega = \{\Omega_{ij}\}$$

where

$$\Omega_{11} = C_p C_y$$
$$\Omega_{12} = -C_p S_y$$
$$\Omega_{13} = S_p$$
$$\Omega_{21} = C_r S_y + S_r S_p C_y$$
$$\Omega_{22} = C_r C_y - S_r S_p S_y$$
$$\Omega_{23} = S_r C_p$$
$$\Omega_{31} = S_r S_y - C_r S_p C_y$$
$$\Omega_{32} = S_r C_y + C_r S_p S_y$$
$$\Omega_{33} = C_r C_p$$
$$C_\alpha = \cos\theta_\alpha;\ S_\alpha = \sin\theta_\alpha,\ (\alpha\varepsilon\{r,p,y\})$$

For $|\theta| \leqq 10$ mrad, $|\sin\theta - \theta| \leqq 0.167\ \mu$rad. Therefore, considering a nominal ERTS altitude of 925 km, it follows that the approximation $\sin\theta \approx \theta$ results in less than one meter of pointing error on the Earth's surface. Similar arguments support neglecting higher-order terms in Ω. On the other hand, for $|\theta_i| \leqq 10$ mrad $(i = 1, 2)$, the usual small-angle approximation $\cos\theta_1 \cos\theta_2 \approx 1$ can result in up to 90 m of pointing error, which is unacceptable. Accordingly, the following small-angle approximation to Ω is employed:

$$R = \begin{bmatrix} C_p C_y & -\theta_y & \theta_p \\ \theta_y & C_r C_y & -\theta_r \\ -\theta_p & \theta_r & C_r C_p \end{bmatrix} \tag{7}$$

The local orbit-based coordinate axes **R**, **P**, **Y** are defined in terms of the ERTS ephemeris time-series vector $\boldsymbol{\sigma} = (\mathbf{R}_S{}^T, \mathbf{V}_S{}^T)^T$, where $\mathbf{R}_S$ is the ERTS ECR position vector, and $\mathbf{V}_S$ is the ERTS ECR velocity vector. (In Appendix A, it is shown how $\boldsymbol{\sigma}$ is obtained from BIAT data for a given scanning session.) In particular,

$$\mathbf{Y} = -\mathbf{R}_S/\|\mathbf{R}_S\|\,;\ \mathbf{R} = \mathbf{V}_S/\|\mathbf{V}_S\|\,;\ \mathbf{P} = \mathbf{Y}x\mathbf{R}$$

where (x) is the vector cross-product operator.§ Any vector referenced to the local orbit-based coordinates can be mapped into the ECR system by applying the unitary transformation matrix

$$E(\boldsymbol{\sigma}, t) = [\mathbf{R}\,\vdots\,\mathbf{P}\,\vdots\,\mathbf{Y}] \tag{8}$$

The mirror scan angle time-series β is defined in terms of the scan profile for a given scan and certain timing parameters associated with the MSS mechanism. A detailed description of β is presented in Appendix B. The deployment angle—which is a function of the image scan line in which the GCP appears—is also defined in Appendix B.

III. Local Linearization of G

The preceding discussion—in particular, Eqs. (2)–(8) and Appendixes A and B—completely defines the transformation **G** in Eq. (1). It remains to find a local linearization of **G** as this is required to define the optimum filter weight in the estimation equations to be given in Sec. IV. Again, it is most convenient to work initially with $\boldsymbol{\theta}$ and hence **g**. The local linearization of **g** about the nominal $\boldsymbol{\theta}$ is found using the matrix partial differentiation operator,

$$\nabla_q = \left[\frac{\partial}{\partial q_1}, \ldots, \frac{\partial}{\partial q_n}\right]^T$$

whose properties are summarized in Van Trees.[5] In point of fact, for $\boldsymbol{\theta}$ in a suitably small neighborhood of $\boldsymbol{\theta}_o$,

$$\mathbf{g}(\boldsymbol{\theta}; \boldsymbol{\sigma}, \beta, t, \phi) \approx \mathbf{g}_o + h(\boldsymbol{\theta}_o; \boldsymbol{\sigma}, \beta, t, \phi)(\boldsymbol{\theta} - \boldsymbol{\theta}_o) \tag{9}$$

where

$$\mathbf{g}_o = \mathbf{g}(\boldsymbol{\theta}_o; \boldsymbol{\sigma}, \beta, t, \phi) \tag{10}$$
$$h(\boldsymbol{\theta}; \boldsymbol{\sigma}, \beta, t, \phi) = [\nabla_\theta \mathbf{g}^T]^T \tag{11}$$

§ In general, orbital ellipticity requires the system **R**, **P**, **Y** to be orthogonalized by applying the Gram-Schmidt algorithm to **Y**, **R** prior to computing **P**. However, the negligible eccentricity of the essentially circular ERTS orbit makes this step unnecessary.

Since $\boldsymbol{\sigma}$ is independent of $\boldsymbol{\theta}$,

$$\nabla_\theta \mathbf{g}^T = \delta \nabla_\theta \mathbf{u}^T + [\nabla_\theta \delta]\mathbf{u}^T \tag{12}$$

where

$$\nabla_\theta \delta = (1 + \mathbf{u}^T \mathbf{R}_S / (\|\mathbf{R}_G\|^2 - \|\mathbf{R}_S\|^2 + (\mathbf{u}^T \mathbf{R}_S)^2)^{1/2})[\nabla_\theta \mathbf{u}^T]\mathbf{R}_S \tag{13}$$
$$\nabla_\theta \mathbf{u}^T = [\nabla_\theta (R\mathbf{1})^T] E^T \tag{14}$$
$$\nabla_\theta (R\mathbf{1})^T = \{a_{ij}\} \tag{15}$$

$$a_{11} = a_{22} = a_{33} = 0$$
$$a_{12} = -S_r C_y S_\beta C_\phi - C_\beta C_\phi$$
$$a_{13} = -S_r C_p C_\beta C_\phi + S_\beta C_\phi$$
$$a_{21} = -S_p C_y S_\phi + C_\beta C_\phi$$
$$a_{23} = -C_r S_p C_\beta C_\phi - S_\phi$$
$$a_{31} = -C_p S_y S_\phi - S_\beta C_\phi$$
$$a_{32} = -C_r S_y S_\beta C_\phi + S_\phi$$
$$C_\alpha = \cos\theta_\alpha(t);\ S_\alpha = \sin\theta_\alpha(t),\ (\alpha\varepsilon\{r,p,y\})$$
$$C_\beta = \cos\beta(t);\ S_\beta = \sin\beta(t)$$
$$C_\phi = \cos\phi;\ S_\phi = \sin\phi$$

The local linearization of **G** about the nominal $\boldsymbol{\Psi}_o$ is given by

$$\mathbf{G}(\boldsymbol{\Psi}; \boldsymbol{\sigma}, \beta, t, \phi) \approx \mathbf{G}_o + H(\boldsymbol{\Psi}_o; \boldsymbol{\sigma}, \beta, t, \phi)(\boldsymbol{\Psi} - \boldsymbol{\Psi}_o) \tag{16}$$

where

$$\mathbf{G}_o = \mathbf{G}(\boldsymbol{\Psi}_o; \boldsymbol{\sigma}, \beta, t, \phi) \tag{17}$$
$$H(\boldsymbol{\Psi}; \boldsymbol{\sigma}, \beta, t, \phi) = [\nabla_\Psi \mathbf{G}^T]^T \tag{18}$$

From Eq. (2) it follows that the (i,j) entry of the matrix H is related to the matrix h according to

$$H_{ij} = h_{i,k_n(j)}\, t^{(j-1) \bmod (n+1)}$$

where

$$k_n(j) = \lfloor (j-1)/(n+1) \rfloor + 1$$

and where $\lfloor x \rfloor$ = greatest integer not exceeding real x, and n = order of the polynomial model for each attitude component. It is assumed that the polynomial models for each of the attitude components are of the same order.

IV. Mean-Square-Sense Optimal Estimator

It can be shown that **G** behaves linearly in a neighborhood of the nominal attitude time series. We are therefore assured by Bucy and Joseph[6] that the following estimator, $\hat{\boldsymbol{\Psi}}$, is optimal in the mean-square sense:

$$\hat{\boldsymbol{\Psi}}(k+1) = \hat{\boldsymbol{\Psi}}(k) + A(k+1)[\mathbf{R}_G(t_{k+1}) - \mathbf{G}(\hat{\boldsymbol{\Psi}}(k); \boldsymbol{\sigma}, \beta, t_{k+1}, \phi_{k+1})] \tag{19}$$

where

$$A(k+1) = P(k+1)H^T \Lambda^{-1}(k+1) \tag{20}$$
$$P(k+1) = P(k) - P(k)H^T[HP(k)H^T + \Lambda(k+1)]^{-1} HP(k) \tag{21}$$
$$H = H(t_{k+1}|k) = H(\hat{\boldsymbol{\Psi}}(k); \boldsymbol{\sigma}, \beta, t_{k+1}, \phi_{k+1}) \tag{22}$$
$$\Lambda(k+1) = E[\mathbf{n}(t_{k+1})\mathbf{n}^T(t_{k+1})] \tag{23}$$
$$P(0) = E[\hat{\boldsymbol{\Psi}}(0)\hat{\boldsymbol{\Psi}}^T(0)] \tag{24}$$
$$\hat{\boldsymbol{\Psi}}(0) = \text{prior estimate of } \boldsymbol{\Psi} \tag{25}$$

V. Implementation Procedure

The estimator $\hat{\boldsymbol{\Psi}}$ was implemented on the CDC 6500 computer using data derived from the NASA-supplied BIAT 1068-35 corresponding to the Baltimore/Washington scene 1062-15190. GCPs in this image were selected from a list supplied by the U.S. Geological Survey. Additionally, USGS provided sections of 7.5 min quadrangle maps showing each GCP's location relative to neighboring features. By comparing these map sections with subimage reproductions of the bulk image it was possible to determine the bulk image line/pixel coordinates of each GCP to within $\pm$ 1 pixel. Using this data, GCP imaging times, t_k, were computed in accordance with

$$t_k = T_{SCAN}(l_k) + T_{\text{SAMPLE}}(p_k) \tag{26}$$

where $T_{\text{SCAN}}(l_k)$ = ICT time at which the scan containing line l_k commences, and $T_{\text{SAMPLE}}(p_k)$ = time *duration* from scan start

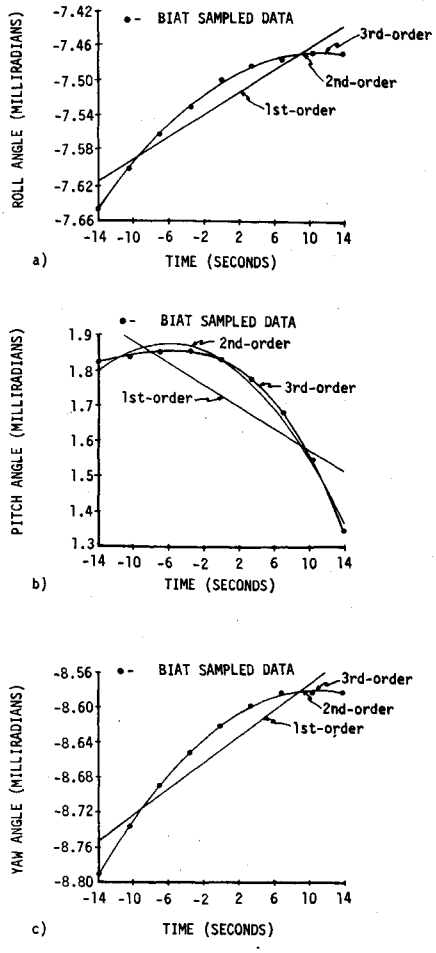

Fig. 2 Attitude time-series models.

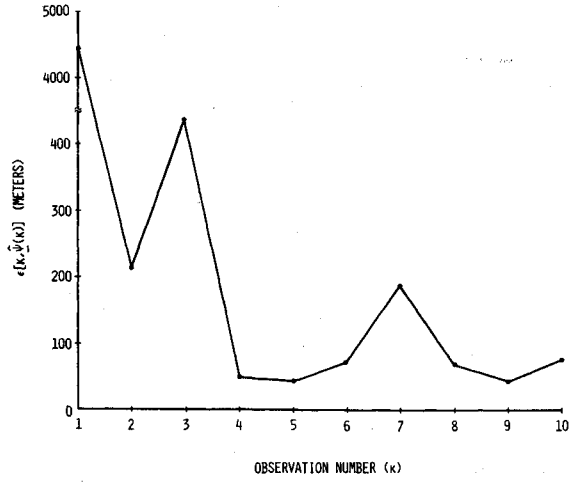

Fig. 3 GCP position estimation error profile.

of l_k to the instant pixel p_k is sampled. Details concerning the computation of T_{SCAN}, T_{SAMPLE}, the detector deployment angle, ϕ_k, and the MSS mirror scan angle time-series, β, can be found in Appendix B. The ephemeris time series, σ, was obtained from ERTS nadir trajectory and altitude sampled data on the BIAT. See Appendix A for the details of this computation.

Inputs to the estimator consisted of ECR vector realizations of the GCPs. The kth GCP's ECR coordinates were computed from precision USGS latitude/longitude coordinates as follows:

$$\begin{aligned}(\mathbf{R}_G)_x(t_k) &= \rho_G(k)\cos\lambda_k\cos\nu_k\\ (\mathbf{R}_G)_y(t_k) &= \rho_G(k)\cos\lambda_k\sin\nu_k\\ (\mathbf{R}_G)_z(t_k) &= \rho_G(k)\sin\lambda_k\end{aligned} \tag{27}$$

where λ_k = geocentric latitude of the kth GCP, ν_k = longitude of the kth GCP, $\rho_G = \rho(1-\varepsilon^2\sin^2\lambda_k)^{1/2}$, ρ = equatorial radius of the earth, and ε = eccentricity of the earth.

The prior estimate of Ψ was derived from attitude sampled-data on the BIAT. Figure 2 shows the results of least-squares fitting 1st, 2nd, and 3rd order polynomials to each set of sampled data. These figures demonstrate the sufficiency of a third-order polynomial representation for each of the attitude components. Accordingly, Ψ was chosen to be twelve dimensional, thus making $\hat{\Psi}$ twelve dimensional

Because statistics for Ψ and $\mathbf{n}(t_k)$, $k = 1, 2, \ldots$, were unavailable, a priori covariance matrix $P(0)$ and the observation noise covariance matrices $\Lambda(k)$, $k = 1, 2, \ldots$, were assigned on a subjective basis. The selection of $P(0)$ was circumscribed by the following assumptions: 1) The components of Ψ are uncorrelated. 2) The uncertainty in the zeroth order component of $\Psi_\alpha(\alpha\varepsilon\{r, p, y\})$ is bounded by the attitude measurement uncertainty specified by NASA (1.22173 mrad). 3) Uncertainty in the jth order component of $\Psi_\alpha(j = 1, 2, 3;\ \alpha\varepsilon\{r, p, y\})$ does not exceed 10% of the absolute value of the component's initial value. On the basis of these assumptions, $P(0)$ was taken to be diagonal with

$$[P(0)]_{ii} = S^2_{(i-1)\bmod(4)+1} \qquad i = 1, 2, \ldots, 12$$

where

$$S_1 = 1.22173 \times 10^{-3},\ S_2 = 10^{-7},\ S_3 = 10^{-8},\ S_4 = 10^{-10}$$

The covariance matrices $\Lambda(k)$, $k = 1, 2, \ldots$, were also taken to be diagonal, reflecting a belief that the components of $\mathbf{R}_G$ are uncorrelated. Furthermore, it was assumed that equal uncertainties are associated with the components of $\mathbf{R}_G$, i.e.,

$$[\Lambda(k)]_{ii} = \xi^2(k), \qquad i = 1, 2, 3$$

For GCPs not obscured by cloud cover, ξ was assigned a value of 30 m. Other GCPs were assigned larger values of ξ commensurate with their definitional uncertainties.

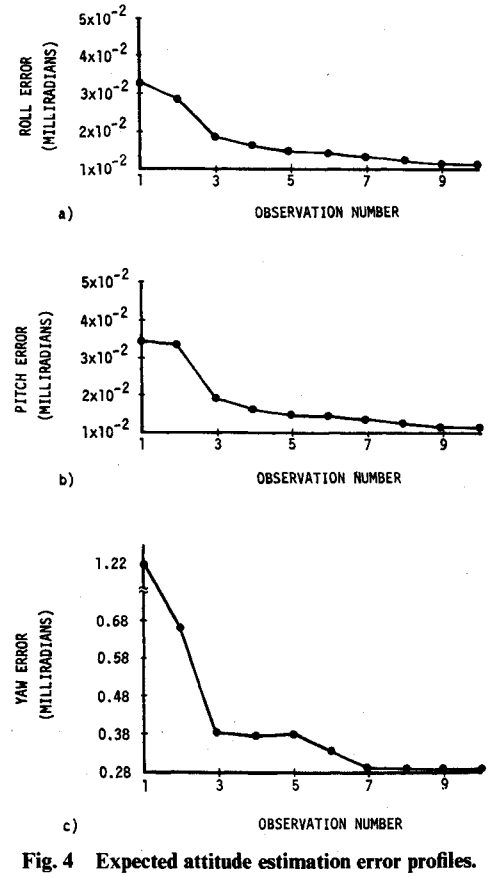

Fig. 4 Expected attitude estimation error profiles.

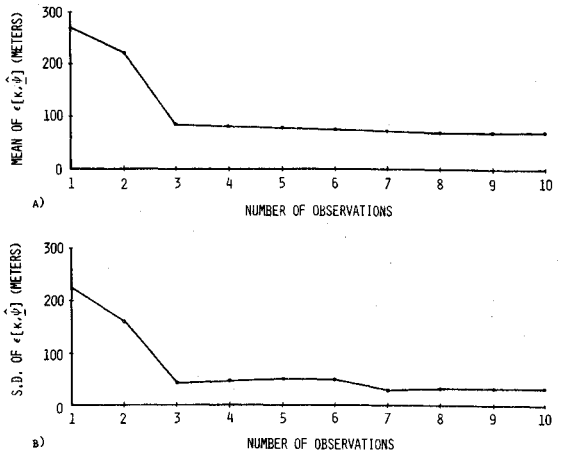

Fig. 5 Mean and standard deviations of position estimation error vs number of observations. Statistics based upon a sample of 10 observations.

VI. Performance Characteristics

The norm of the position estimation error,

$$\varepsilon_p(k,\Psi) = \|\mathbf{R}_G(t_k) - \mathbf{G}(\Psi;\sigma,\beta,t_k,\phi_k)\|$$

where $\mathbf{R}_G(t_k)$ is computed according to Eq. (27), is a useful measure of the estimator's stability. Intuitively, one expects a decreasing trend in $\varepsilon_p[k,\hat{\Psi}(k-1)]$ vs k if $\hat{\Psi}$ is stable; and, indeed, Fig. 3 bears out this behavior for the ten GCPs selected.

Another measure of $\hat{\Psi}$'s stability is the behavior of the zeroth-order error-covariance terms, P_{11}, P_{55}, and P_{99}, as a function of observation number. Plots of the square roots of these functions (cf. Fig. 4) exhibit a highly stable monotone decreasing behavior which tends to be asymptotic. Notice that after 10 stages, the expected roll and pitch estimates have converged to within ± 0.01 milliradians of their true values, whereas the expected yaw estimate converges to within ± 0.28 mrad of its true value. The large uncertainty for yaw is most likely because position errors are less sensitive to yaw than to pitch and roll.

The accuracy of the estimator as a function of the number of observations performed is summarized by Fig. 5. The plots shown were obtained by running the estimator with $k = 1, 2, \ldots,$ 10 observations. After the kth observation, the resultant estimate $\hat{\Psi}(k)$ was used to compute $\varepsilon_p[j,\hat{\Psi}(k)]$ for $j = 1, 2, \ldots, 10$. From this sample of size ten, a mean and standard deviation were computed. By repeating this process for $k = 1, 2, \ldots, 10$, the plots in Fig. 5 were generated. The reason that only three GCP observations are required to correct the attitude time-series to within the MSS's resolutional capability is that, for the image considered, the attitudinal uncertainty is essentially time-invariant. This is evident when one compares the 1st, 2nd, and 3rd order coefficients of the a priori and 10-GCP-optimal estimates of $\Psi_\alpha, \alpha\varepsilon\{r,p,y\}$, in Table 1.

VII. Conclusions

It has been shown how mean-square-sense optimal estimation theory can be successfully applied to the ERTS/MSS image rectification problem. For a typical ERTS scene, a priori position estimation uncertainties on the order of 4 km have been reduced to 80 m by employing ground control point observables to drive a sequential attitude time-series estimator. By virtue of its sequential structure, the estimator developed here provides the capability to assess the accuracy of a control point before it is used. Moreover, as position estimation errors are diminished at each stage, it becomes increasingly easier to locate a control point in the image. This feature is of paramount importance in operational systems where high throughput is required.

Although the attitude time-series estimator described herein was developed in the context of the ERTS system, its design is sufficiently general to be applicable to other optically scanned spaceborne imaging systems.

Appendix A: Computation of the ERTS Ephemeris Time-Series

The BIAT contains certain ICT sampled-data necessary to compute the ERTS ephemeris time-series relative to each scanning session. For a given scanning session, this data consists of nadir trajectory geodetic latitude/longitude and altitude samples, as well as the spacecraft heading angle at ICT zero. Time-series (restricted to an image time interval) for altitude and nadir latitude/longitude are obtained by fitting polynomials of suitable order to the samples in each data set.¶ However, prior to computing the latitude time-series polynomial, the geodetic latitude samples $\{\lambda'_k\}$ are converted to geocentric latitude samples $\{\lambda_k\}$ using the relationship

$$\lambda_k = \tan^{-1}[(1-\varepsilon^2)\tan\lambda'_k]$$

where ε is the eccentricity of the oblate spheroid Earth model. This conversion facilitates the expression of ECR vector coordinates in terms of spherical coordinate formulas.

The distance at ICT t between the Earth center and the ERTS nadir is given by

$$\rho_G(t) = \rho[1-\varepsilon^2\sin^2\lambda(t)]^{1/2}$$

where ρ is the Earth's equatorial radius and λ is the geocentric latitude time series.** Letting h denote the altitude time series, it follows that

$$\|\mathbf{R}\|(t) = \rho_G(t) + h(t)$$

is the distance at ICT t between the Earth center and the ERTS. Taking into account the geocentric latitude $\lambda(t)$ and longitude $\phi(t)$ of the spacecraft nadir at ICT t, the ERTS ECR position vector $\mathbf{R}(t)$ is obviously given by

$$\mathbf{R}(t) = [R_x(t), R_y(t), R_z(t)]$$

where

$$R_x(t) = \|\mathbf{R}\|(t)\cos\lambda(t)\cos\phi(t)$$
$$R_y(t) = \|\mathbf{R}\|(t)\cos\lambda(t)\sin\phi(t)$$
$$R_z(t) = \|\mathbf{R}\|(t)\sin\lambda(t)$$

The ERTS ECR velocity vector can be derived in terms of the nadir geocentric latitude/longitude and spacecraft heading time-series. Since only one heading sample is given on the BIAT for

Table 1 Optimal attitude coefficient vectors[a,b]

Stage	0 (a-priori)	5	10
Ψ_r	−7.50346006E-03	−7.91632403E-03	−7.92132188E-03
	6.16945072E-06	6.17298849E-06	6.17216580E-06
	−2.83605404E-07	−2.83238413E-07	−2.83019062E-07
	9.37544491E-10	9.37440772E-10	9.37288552E-10
Ψ_p	1.83105432E-03	6.96552787E-03	6.95558790E-03
	−1.03662074E-05	−1.03488534E-05	−1.03600776E-05
	−1.28142498E-06	−1.28270303E-06	−1.28214238E-06
	−3.53211885E-08	−3.53191831E-08	−3.53199302E-08
Ψ_y	−8.62098473E-03	−2.31298765E-03	−1.25039820E-03
	7.63411074E-06	7.63423736E-06	7.63416607E-06
	−3.44625591E-07	−3.44598980E-07	−3.44606009E-07
	−1.09426592E-09	−1.09427277E-09	−1.09427828E-09

[a] Attitude expressed in units of radians.
[b] XEN denotes the number $(X)(10^N)$.

¶ For the image considered in this study (BIAT 1068-35, Scene 1062-15190), third-order least-squares polynomials were found to be sufficient.

** The norm of the kth GCP's ECR position vector can be approximated by $\rho_G(t_k)$, where t_k is the GCP imaging time.

each scene, the heading angle time-series (restricted to a given scene) is assumed to be constant. The heading angle γ is measured with respect to an ECR vector $\mathbf{Q}$ whose defining properties are:

$$\mathbf{Q}(t)^T\mathbf{R}(t) = 0$$
$$[\mathbf{Q}(t)+\mathbf{R}(t)]^T\mathbf{X} = 0$$
$$[\mathbf{Q}(t)+\mathbf{R}(t)]^T\mathbf{Y} = 0$$

where $\mathbf{X}$ and $\mathbf{Y}$ are the x and y basis vectors, respectively, in the ECR system. Since the ERTS orbit is circular, the ERTS ECR velocity vector $\mathbf{V}$ can be found by rotating a unit vector in the direction of $\mathbf{Q}$ through an angle γ in the hyperplane defined by $\mathbf{R}$ and the origin. This is achieved by first referring $\mathbf{Q}$ to a new coordinate system ($\mathbf{X}'$, $\mathbf{Y}'$, $\mathbf{Z}'$) such that

$$\mathbf{Z}' = \mathbf{Q}/\|\mathbf{Q}\|\,;\ \mathbf{Y}' = \mathbf{R}/\|\mathbf{R}\|\,;\ \mathbf{X}' = \mathbf{R}\times\mathbf{Q}/\|\mathbf{R}\times\mathbf{Q}\|$$

A unit vector in the primed system along $\mathbf{Q}$'s direction is described by $\mathbf{1}' = (0,0,1)^T$. The clockwise rotation of $\mathbf{1}'$ about the y' axis and through an angle γ results in

$$\mathbf{1}'_\gamma = (-\sin\gamma, 0, \cos\gamma)^T$$

which is a unit vector in the direction of the ERTS velocity vector relative to the primed system. An ECR unit vector in the direction of $\mathbf{V}$ is obtained by mapping $\mathbf{1}'_\gamma$ into the ECR system using the unitary matrix

$$T = [\mathbf{R}\times\mathbf{Q}\,\vdots\,\mathbf{R}\,\vdots\,\mathbf{Q}]$$

Thus,

$$\mathbf{V}(t)/\|\mathbf{V}\| = T(t)\mathbf{1}'_\gamma$$
$$= \begin{bmatrix} -\sin\phi(t)\sin\gamma - \cos\phi(t)\sin\lambda(t)\cos\gamma \\ \cos\phi(t)\sin\gamma - \sin\phi(t)\sin\lambda(t)\cos\gamma \\ \cos\lambda(t)\cos\gamma \end{bmatrix}$$

Appendix B: Properties of the ERTS Multispectral Scanner

The ERTS Multispectral Scanner (MSS) was designed to record imagery in four spectral bands. A total of 24 detectors—six per spectral band—are deployed in a matrix pattern. For a given spectral band, one scan of the MSS mirror produces simultaneously six contiguous lines of an analog bulk image. A total of 2340 lines (390 scans) constitute one such image. The bulk images supplied by NASA contain line-length-corrected digitized versions of the analog images. Each digitized line consists of N_p pixels which are obtained by sampling at 9.8 μsec intervals. Each pixel corresponds to a 79 m × 79 m region on the ground.

The detector matrix pattern is situated in a plane parallel to the plane formed by the x and y spacecraft body coordinate axes. Therefore, the position of each detector in a given spectral band can be described by a deployment angle $\psi_j, j = 1, 2, \ldots, 6$, which can be calculated from the dimensions of the detector matrix pattern and the focal length of the scanner optical system. These angles are taken clockwise in the x-z body axis plane and with respect to the positive z axis.

If l_k is the scan line in which the kth GCP is imaged, the detector which recorded that line is deployed at an angle

$$\phi_k = \psi_{(l_k-1)} \bmod (6)+1$$

The ICT imaging time t_k is determined from the bulk image line/pixel coordinate (l_k, p_k) of the kth GCP. In particular,

$$t_k = T_{\text{SCAN}}(l_k) + T_{\text{SAMPLE}}(p_k)$$

where

$$T_{\text{SCAN}}(l_k) = T_{196} - L_{196}(l_k)T_S$$
$$T_{\text{SAMPLE}}(p_k) = (p_k-1)T_p$$
$$T_{196} = T_S/2 - (N_P-1)T_P/2$$
$$L_{196}(l_k) = 196 - \lfloor (l_k-1)/6 \rfloor + 1$$

and where T_S = time duration of a complete scan and retrace, T_P = duration of time required to sample 1 pixel, and N_P = number of pixels sampled in one line.

The MSS mirror scan angle $\beta'(t')$ corresponding to the time duration t' after line start is given by

$$\beta'(t') = P_S(t'_{\text{mid}}) - P_S(t')$$
$$P_S(t) = A\sin(Wt+B)+C$$

where $A = 0.384045$ rad, $B = -0.251320$ rad, $C = 0.095505$ rad, $W = 16.5248$ rad/sec, and $t'_{\text{mid}} = 0.016035$ = time duration from line start to midscan. Therefore, all that is required to compute the mirror scan angle $\beta(t_k)$ at ICT t_k is the time duration from line start to the instant when the sampling of pixel p_k commences. This time duration is, by definition, $T_{\text{SAMPLE}}(p_k)$. Thus

$$\beta(t_k) = \beta'[T_{\text{SAMPLE}}(p_k)]$$

References

[1] Rifman, S., "Digital Rectification of ERTS Multispectral Imagery," *Proceedings of the Symposium on Significant Results Obtained from the ERTS-1*, Vol. I, Sec. B, March 1973, pp. 1131–1142, NASA.

[2] *ERTS Data Users Handbook*, Doc. 71SD4249, NASA.

[3] Thomas, V. L., "Generation and Physical Characteristics of ERTS MSS System Corrected Computer Compatible Tapes," Doc. X-563-73-206, July 1973, NASA.

[4] *ERTS Data Users Handbook*, Doc. 71SD4249, Appendix B, p. B1, NASA.

[5] Van Trees, H. L., *Detection, Estimation and Modulation Theory, Part I*, Wiley, New York, 1968, p. 150.

[6] Bucy, R. and Joseph, P., *Filtering for Stochastic Processes with Applications to Guidance*, Interscience, New York, 1968, pp. 143–145.